

RSC Advances



This is an *Accepted Manuscript*, which has been through the Royal Society of Chemistry peer review process and has been accepted for publication.

Accepted Manuscripts are published online shortly after acceptance, before technical editing, formatting and proof reading. Using this free service, authors can make their results available to the community, in citable form, before we publish the edited article. This *Accepted Manuscript* will be replaced by the edited, formatted and paginated article as soon as this is available.

You can find more information about *Accepted Manuscripts* in the [Information for Authors](#).

Please note that technical editing may introduce minor changes to the text and/or graphics, which may alter content. The journal's standard [Terms & Conditions](#) and the [Ethical guidelines](#) still apply. In no event shall the Royal Society of Chemistry be held responsible for any errors or omissions in this *Accepted Manuscript* or any consequences arising from the use of any information it contains.

Cite this: DOI: 10.1039/c0xx00000x

www.rsc.org/xxxxxx

ARTICLE TYPE

A “Green” High-initiation-power Primary Explosive: Synthesis, 3D Structure and Energetic Properties of Dipotassium 3,4-Bis(3-dinitromethylfuran-4-oxy)furan

Lianjie Zhai,^a Xuezhong Fan,^{*a} Bozhou Wang,^a Fuqiang Bi,^a Yanan Li^{a,b} and Yanlong Zhu^a

Received (in XXX, XXX) 15th May 2015, Accepted Xth XXXXXXXX 2015
DOI: 10.1039/b000000x

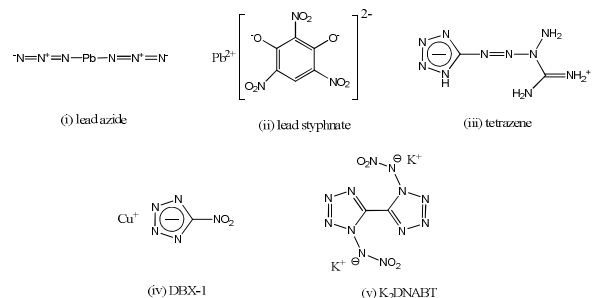
A new green primary explosive, dipotassium 3,4-bis(3-dinitromethylfuran-4-oxy)furan (K₂BDFOF), was synthesized via a four-step procedure including cyano addition, diazotization, N₂O₅ nitration, and KI reduction. The compound was characterized by multinuclear NMR spectroscopy, IR spectroscopy, elemental analysis, DSC, TG/DTG as well as single crystal X-ray diffraction. X-ray diffraction studies reveal an intriguing 3D framework structure. The central K ions are linked by dinitromethanide anions to give a 1D spiral chain with parallelogram-like repeat units, and these 1D chains are further linked by one oxygen atom in the nitro group coordinated with K ion to form a two-dimensional wave-like layer structure. Additionally the kinetic parameters of the exothermic process for K₂BDFOF were studied by Kissinger's and Ozawa–Doyle's methods. The sensitivities were determined by standardised impact and friction tests, and the heat of formation was calculated with the atomization method at the CBS-4M level of theory. With the heat of formation (-8.4 kJ mol⁻¹) and the room-temperature X-ray density (2.09 g cm⁻³), impressive values for the detonation parameters such as detonation velocity (8431 m s⁻¹) and pressure (329 kbar) were computed using the EXPLO5 program and compared to the most commonly used primary explosive lead azide as well as recently published dipotassium 1,1'-dinitramino-5,5'-bistetrazolate.

1 Introduction

Primary explosives form a group of explosives that upon ignition undergo a deflagration-to-detonation transition (DDT), generating a shockwave capable of initiating detonation in a secondary explosive.¹⁻⁴ The main requirement for these explosives is a sufficient sensitivity to the initiating stimuli, the most often used being impact, friction, stab, heat, static electricity, flame etc. In view of the fact that primary explosives are widely used in detonators, primers, blasting caps, and initiators for a variety of military purposes and civilian applications, the continuous research toward new green primary explosives has been the focus of several research groups worldwide for a long time. During this time many new chemical substances with properties of primary explosives have been synthesized but only a few of them have been evaluated as promising candidates as a lead azide replacement.⁵⁻⁸

The most commonly used primary explosives are lead azide, lead styphnate, and tetrazene (Scheme 1).⁹⁻¹¹ Lead azide is usually used as a neat material in a transfer charge in detonators or in formulations for stab initiation mix or primer mixes as it is easier to initiate. This primary explosive is very sensitive to impact and friction and cannot be dead pressed even at relatively low pressures; its drawback is unstable in the presence of oxidizing agents and ammonia.¹² Lead styphnate is used in

formulations with lead azide for primer and initiation mixes and rarely found as a neat material in applications due to its poor initiator for detonation.



Scheme 1 Molecular structures of common primary explosives.

Further, lead-based primary explosives are well established to cause environmental and health related problems. Lead is both an acute and chronic toxin, and the human body has difficulty in removing it once it has been absorbed and dissolved in the blood.¹ Thus, there is a need to develop “green” primary explosives, to replace lead-based compounds. Silver-containing primary explosives may be suitable candidates as a lead azide replacement for practical application that fulfilled most criteria for practical applications nowadays.^{6, 13-14} Although silver salts often show the best energetic performance of the metal cations, they also bear some problems that make them unfeasible for commercial applications. These often include a sensitivity to

light, a high price, and the toxicity of silver toward microorganisms and aquatic life.¹⁵ Further employable cations include the alkali metals cesium or transition metals like copper (DBX-1, Scheme 1 (iv)).^{13,16-17} However, it should be mentioned that copper (II) is also toxic to microorganisms,¹⁸ but to a lesser degree than silver and is therefore not yet desirable.

A recently employed idea is the formation of nontoxic metal complexes containing potassium instead of toxic heavy metals. As is already known, K exhibits a good coordination ability to different kinds of ligands, and more importantly, is an environmentally-friendly ion compared to heavy metal ions such as lead, mercury and silver. To date, numerous energetic potassium salts have been synthesized and characterized in the literature.^{6, 19-21} Of particular interest are dipotassium 1,1'-dinitramino-5,5'-bistetrazolate (K_2 DNABT, Scheme 1 (v)) which was developed by Klapötke's team last year.²² They have found that K_2 DNABT outperforms lead azide in detonation tests and is similar to lead azide in terms of sensitivities, such as impact, friction, and electrostatic discharge. What's more, the compound possesses high thermal stability, resisting decomposition when held at 100 °C for 48 hours. It seems a perfect candidate as a lead azide replacement for practical application nowadays.

In the present work, we focus our attention on the high energy of the furazanyl ethers that fulfill many requirements in the challenging field of energetic materials research. When a bridged oxygen atom is introduced into furazan, it could be significantly increase both the density and thermal stability of the molecule.²³⁻²⁵ Thus, furazanyl ether compounds have been studied over the last couple of years with growing interest, and numerous compounds with promising properties as energetic materials have been reported, such as 3,3'-dinitrodifurazanyl ether, oxy-bridged bis(1*H*-tetrazol-5-yl)furazan, 3,3'-bis (nitro-*NNO*-azoxy)-difurazanyl ether, bifurazano[3,4-*b*:3',4'-*f*] furoxano [3'',4''-*d*] oxacycloheptatriene etc.²⁵⁻²⁸ Additionally, introducing furazanyl ether as backbone into dinitromethide group could be an effective method because of its advantages, such as its variety of coordination modes, high oxygen content and explosive properties. A good example is the previously synthesised anion 3,3'-bis(dinitromethide) difurazanyl ether, which shows remarkable high densities of its salts.²⁹

In our continuing efforts to seek more powerful and eco-friendly primary explosives, we present here the synthesis and characterization of a new primary explosive dipotassium 3,4-bis(3-dinitromethylfurazan-4-oxy)furazan (K_2 BDFOF), which only contains potassium as the metal and is also an alternative to lead azide. Since containing the dinitromethyl moiety, K_2 BDFOF shows considerably higher oxygen balance, detonation pressure and velocity, compared to the rich-nitrogen compound K_2 DNABT. Additionally, X-ray crystallographic measurements were performed and deliver insight into structural characteristics of the 3D framework. The potential application of the compound as primary explosive was studied and evaluated using the experimentally obtained values for the thermal decomposition and the sensitivity data as well as the calculated detonation parameters.

2 Experimental

CAUTION! Compounds **4** and K_2 BDFOF are highly powerful energetic materials that show increased sensitivities towards various stimuli. Proper protective measures (safety glasses, face shield, leather coat, and ear plugs, etc.) should be used when synthesizing and handling these compounds, especially when compound K_2 BDFOF is prepared on a larger scale.

2.1 Instruments and conditions

Elemental analyses (C, H and N) were performed on a VARI-EL-3 elementary analysis instrument. Infrared spectra were obtained from KBr pellets on a Nicolet NEXUS870 Infrared spectrometer in the range of 4000–400 cm^{-1} . 1H NMR and ^{13}C NMR were obtained in DMSO- d_6 on a Bruker AV500 NMR spectrometer. The DSC experiment was performed using a DSC-Q200 apparatus (TA, USA) under a nitrogen atmosphere at a flow rate of 50 mL min^{-1} . About 0.3 mg of the sample was sealed in aluminum pans for DSC. The TG/DTG experiment was performed using a SDT-Q600 apparatus (TA, USA) under a nitrogen atmosphere at a flow rate of 50 mL min^{-1} . The sensitivity to impact stimuli was determined by fall hammer apparatus, applying a standard staircase method using a 2 kg drop weight. The friction sensitivity of the compound was determined using a Julius Peters apparatus, following the BAM method.³⁰ The sample used for each test is about 20 mg.

2.2 Computational Details

All quantum chemical calculations were carried out using the Gaussian 09 (Revision A.02) program package and visualized by GaussView 5.05.³¹⁻³² The enthalpies (H°) and free energies (G°) were calculated using the complete basis set method (CBS-4M) based on X-ray diffraction data, in order to obtain accurate.³³⁻³⁴ The CBS models use the known asymptotic convergence of a pair of natural orbital expressions to extrapolate from calculations using a finite basis set to the estimated complete basis set limit. CBS-4 starts with a HF/3-21G(d) structure optimization, which is the initial guess for the following self-consistent field (SCF) calculation as a base energy and a final MP2/6-31+G calculation with a CBS extrapolation to correct the energy in the second order. The used reparameterized CBS-4M method additionally implements a MP4(SDQ)/6-31+(d, p) calculation to approximate higher order contributions and also includes some additional empirical corrections.³³⁻³⁴ The enthalpies of the gas-phase species were estimated according to the atomization energy method.³⁵⁻³⁶

2.3 X-ray Crystallography

Single crystals suitable for X-ray measurements were obtained by slow evaporation of an aqueous solution of K_2 BDFOF. A yellow grain with dimensions 0.33 × 0.26 × 0.20 mm was used for the X-ray crystallographic analysis. The data were collected on a Bruker SMART Apex II CCD X-ray diffractometer equipped with a graphite-monochromatized MoK α radiation ($\lambda = 0.71073 \text{ \AA}$) using the ϕ - ω scan mode ($2.27 < \theta < 25.08^\circ$). The structure was solved by direct methods and refined by full-matrix least-squares techniques on F^2 using SHELXL-97 programs.³⁷ All non-hydrogen atoms were refined anisotropically. Crystal data and refinement results were summarized in Table 1. CCDC-966224 for contains the supplementary crystallographic data, which can be obtained free of charge from The Cambridge Crystallographic Data Centre

via www.ccdc.cam.ac.uk/data_request/cif.

Table 1 Crystal and structure refinement data for K₂BDFOF

Empirical formula	C ₈ K ₂ N ₁₀ O ₁₃
Formula weight /g mol ⁻¹	522.38
Temperature /K	296(2)
Crystal system	Monoclinic
Space group	C2/c
Crystal size(mm)	0.33 × 0.26 × 0.20
a(Å)	13.2796(19)
b(Å)	6.9892(10)
c(Å)	18.484(3)
α(°)	90
β(°)	104.019(2)
γ(°)	90
V (nm ³)	1.6645(4)
Z	4
D _c (g cm ⁻³)	2.085
Absorption coefficient(mm ⁻¹)	0.675
F(000)	1040
θ range for data collection	2.27 to 25.08
Reflections collected	3992
Independent reflections	1470 [R(int) = 0.0334]
Completeness to 2θ	99.8 %
Data/restraints/parameters	1470 / 0 / 151
Goodness-of-fit on F ²	1.053
Final R indices [I > 2σ(I)]	R ₁ = 0.0358, wR ₂ = 0.0967
R indices (all data)	R ₁ = 0.0475, wR ₂ = 0.1053
Largest diff. peak and hole/e Å ⁻³	0.265 and -0.290

2.3 Syntheses

3,4-Bis(3-aminoximidofurazan-4-oxy)furazan (2): 3,4-Bis(3-cyano-furazan-4-oxy)furazan (5.76 g, 20 mmol) was added to a mixture consisting of water (55 mL) and isopropanol (25 mL), and then sodium carbonate anhydrous (2.23 g, 21 mmol) and hydroxylamine hydrochloride (2.92 g, 42 mmol) was added at ambient temperature. The reaction mixture was stirred further for 2 h at 50 °C. The precipitate was filtered, washed with ice-cold water, and dried in vacuum over P₂O₅ to afford **2** as a white solid. The obtained solid was recrystallized from methanol to furnish the product as white platelets (6.74 g, 91.2%). mp 219–220 °C; ¹H NMR (DMSO-*d*₆, 500 MHz) δ 10.61 (s, 2H, OH), 6.35 (s, 4H, NH₂); ¹³C NMR (DMSO-*d*₆, 125 MHz) δ 159.25, 154.20, 142.29, 141.19; IR (cm⁻¹, KBr) 3503, 3487, 3382, 3276, 2893, 1675, 1595, 1576, 1553, 1523, 1439, 1254, 1175, 1034, 967; Anal. calcd for C₈H₆N₁₀O₇ (%): C 27.13, N 39.55, H 1.71, found C 26.64, N 39.28, H 1.70.

3,4-Bis(3-chloroximidofurazan-4-oxy)furazan (3): Compound **2** (5.31g, 15 mmol) was dissolved in 55 mL of concentrated hydrochloric acid (55 mL) and water (30 mL). Saturated sodium nitrite (2.16 g, 31 mmol) in water (12 mL) was added dropwise to the stirred solution of **2** at 0 °C. After stirring for 2 h, the reaction mixture was heated to 20 °C for 1.5 h until N₂ evolution stopped. The resulting white precipitate was filtered, washed with cold water twice, and dried in vacuum to yield **3** as a white solid. After recrystallization from MeOH/H₂O (V:V = 1:1), 5.40 g (86.3%) colorless crystals of **3** were obtained. mp 82–83°C; ¹H NMR (DMSO-*d*₆, 500 MHz) δ 13.74 (s, 2H, OH); ¹³C NMR (DMSO-*d*₆, 125 MHz) δ 158.26, 153.41, 143.23, 123.30; IR (cm⁻¹, KBr) 3583, 3505, 3346, 2832, 2759, 1701, 1605, 1589, 1560, 1528, 1512, 1423, 1301, 1252, 1028, 943; Anal. calcd for C₈H₂N₈O₇Cl₂ (%): C 24.45, N 28.51, H 0.51, found C 24.23, N 28.19, H 0.85.

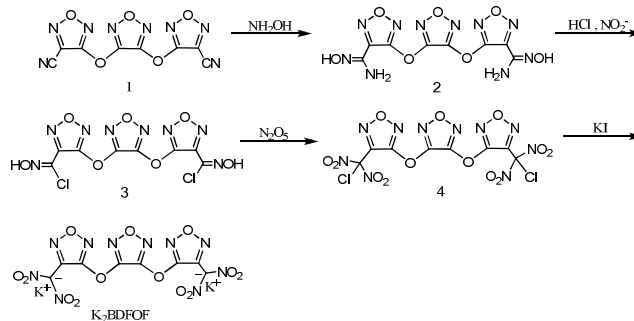
3,4-Bis(3-chlorodinitromethylfurazan-4-oxy)furazan (4): To a suspension of **3** (0.75 g, 1.9 mmol) in CHCl₃ (50 mL) at 15°C was added N₂O₅ (1.63 g, 23 mmol). The mixture was heated to 45°C and kept at this temperature for 40 min. The solvent was evaporated and the residue was subjected to column chromatography on silica gel using ethyl acetate–pentane (V:V = 1:6) as eluent to isolate the pure colorless crystals **4** (0.27 g, 28.0%). mp 79–80°C; ¹³C NMR (DMSO-*d*₆, 125 MHz) δ 159.45, 152.73, 139.27, 113.06; IR (cm⁻¹, KBr) 1602, 1584, 1544, 1501, 1275, 1234, 1030, 981, 816, 786, 621; Anal. calcd for C₈N₁₀O₁₃Cl₂ (%): C 18.66, N 27.19, found C 18.40, N 26.95.

Dipotassium 3,4-bis(3-dinitromethylfurazan-4-oxy)furazan (K₂BDFOF): Compound **4** (1.29 g, 2.5 mmol) was dissolved in MeOH (18 mL) and treated with solution of KI (1.99 g, 12 mmol) in MeOH (22 mL) at room temperature. The resulting mixture was stirred for 1 h and triturated with Et₂O (20 mL). Precipitate was collected, washed with ice-cold water, MeOH, and Et₂O to give a pure product as a yellow solid (1.17 g, 88.9%). T_{dec} 221.5°C; ¹³C NMR (DMSO-*d*₆, 125 MHz) δ 160.54, 153.57, 142.40, 119.58; IR (cm⁻¹, KBr) 1597, 1569, 1552, 1529, 1483, 1312, 1230, 1036, 1000, 743; Anal. calcd for C₈N₁₀O₁₃K₂ (%): C 18.36, N 26.76, found C 18.12, N 26.49.

3 Results and Discussion

3.1 Syntheses

An overview about all syntheses described in this work is depicted in Scheme 2. 3,4-Bis(3-cyanofurazan-4-oxy)furazan (**1**) was prepared according to a known procedure.²⁴ The addition reaction of compound **1** with hydroxylamine leads to pure 3,4-bis(3-aminoximidofurazan-4-oxy)furazan (**2**) in a high yield. 3,4-Bis(3-chloroximidofurazan-4-oxy)furazan (**3**) is obtained by diazotization of compound **2**, using sodium nitrite and concentrated hydrochloric acid. The mixture has been cooled to 0°C and the addition of the sodium nitrite should be carried out slowly to ensure a clean reaction and complete conversion. Lukyanov et al had described the synthesis of chlorodinitromethyl group from chlorooximes by nitration with N₂O₅.^{38–39} Therefore, when **3** was subjected to N₂O₅ in chloroform, 3,4-bis(3-chlorodinitromethylfurazan-4-oxy)furazan (**4**) was formed in a low yield (28%). In order to improve the yield of compound **4**, we tried to change the amount of N₂O₅, reaction temperature and nitration reagent, but all attempts have been unsuccessful. In the last step compound **4** was further reacted with KI/CH₃OH yielding dipotassium 3,4-bis(3-dinitromethylfurazan-4-oxy)furazan (K₂BDFOF) in 88.9% yield. Potassium salt is the most sensitive compound and should be handled with care.



Scheme 2 Synthesis of K_2 BDFOF.

3.2 Crystal structure

Dipotassium 3,4-bis(3-dinitromethylfuran-4-oxy)furan (K_2 BDFOF) crystallizes in the monoclinic space group $C2/c$ with four formula units in the unit cell and a calculated density of 2.09 g cm^{-3} at 296 K. The repeating unit of K_2 BDFOF contains two potassium ions, and one BDFOF anions and shows a symmetry axis through the central furazan ring of BDFOF anions. As shown in Fig. 2, each K ion is eight-coordinated by seven oxygen atoms (O1, O1 v, O2 iv, O3, O3 v, O4 ii, O4 v, symmetry codes as in Figure 2) and one nitrogen atom (N3 ii) from five different BDFOF anions, of which all O atoms are from the nitro group. The K–O bond distances vary from 2.695(2) to 3.021(2) Å with an average distance of 2.852(2) Å, while the K–N bond distance is slightly shorter, 3.059(2) Å. Selected bond lengths and bond angles are shown in Table S1 (see the Supporting Information). The values of C(3)–O(6) [1.368(3) Å] and C(4)–O(6) [1.348(3) Å] are shorter than those of the normal C–O single bond (0.142~0.146 nm); this may be due to the p - π conjugative effect and the electron-withdrawing influence of furazan ring. Delocalization of the negative charge on the entire dinitromethanide anion is evident from these bond lengths combined with the planarity: (a) the C1–N1 [1.390(3) Å] and C1–N2 [1.379(3) Å] bond lengths are much shorter than the average value for a normal C–N single bond but significantly longer than a C=N double bond; (b) a similar trend is observed for the N–O bond of the dinitromethanide anion in BDFOF; (c) the dinitromethanide anion is almost coplanar, which is supported by the torsion angles [O3–N1–C1–N2, $-8.9(4)^\circ$; O4–N1–C1–N2, $169.7(2)^\circ$].

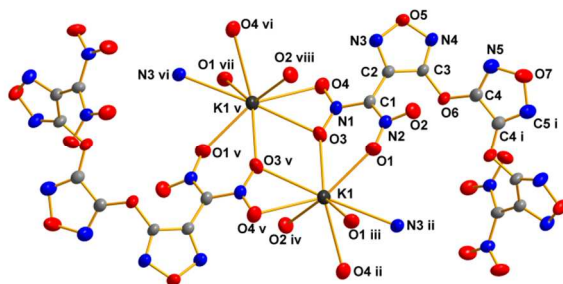


Fig. 1 Molecular structure of K_2 BDFOF with cation coordination. Thermal ellipsoids are drawn at the 50 % probability level. Symmetry codes: (i) $2-x, y, 1.5-z$; (ii) $1/2+x, 1/2+y, z$; (iii) $2-x, 2-y, 1-z$; (iv) $x, 1+y, z$; (v) $3/2-x, 5/2-y, 1-z$; (vi) $1-x, 2-y, 1-z$; (vii) $x-1/2, 1/2+y, z$; (viii) $3/2-x, 3/2-y, 1-z$.

It is noted that a parallelogram-like unit is formed between the two adjacent dinitromethanide anions by two K cations, resulting in a one-dimensional spiral chain extending parallel to the bc plane through the K1–O1 iii bond (Fig. 2). And the coordination action between K1 and O2 atoms from different BDFOF anion, further helps the adjacent spiral chains forming a two-dimensional wave-like layer structure (Fig. 3). Finally, these wave-like two-dimensional layers are linked to form the three-dimensional network structure via N3 and O4 atoms of the BDFOF anion coordinated with K ions (Fig. 4).

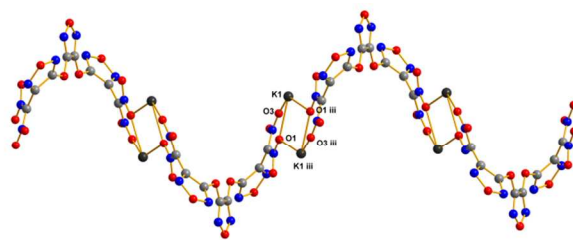


Fig. 2 A view of the one-dimensional spiral chain of K_2 BDFOF along the a axis.

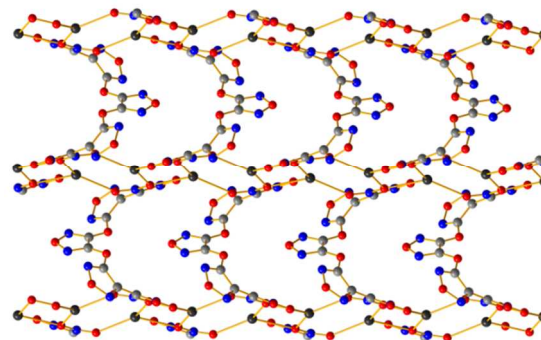


Fig. 3 A view of the two-dimensional wave-like layer structure of K_2 BDFOF.

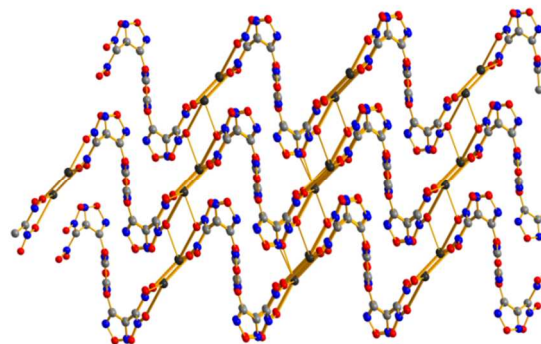


Fig. 4 The extended 3D network based on layers.

3.3 Thermal stability and sensitivities

In order to study the thermal decomposition processes of K_2 BDFOF, the DSC and TG/DTG experiments were carried out with flowing dry oxygen-free nitrogen atmosphere. Fig. 5 shows the DSC curves of the decomposition process of K_2 BDFOF at different heating rates of 5, 10, 15 and 20 K min^{-1} . In the DSC curves, one intense and sharp exothermic process occurs at 210.4°C and ends at 225.7°C with a peak temperature of 221.5°C when the heating rate is 5°C min^{-1} . It was also found that, with the increase of the heating rate, the decomposition temperatures and the exothermic peaks of K_2 BDFOF shifted to higher temperatures. The TG/DTG experiments were carried out under the heating rate of 5°C min^{-1} and the typical TG/DTG curve is shown in Fig. 6. As noticeable from the TG curve, there is one mass-loss stage, corresponding to only one peak in the DSC curve. A sudden weight loss is observed at 217.0°C that stops at 224.6°C , accompanied by about 98.6% mass loss, which is more

than the expected mass for the remaining potassium oxide (K_2O) as solid residues. Through the explosion that releases a huge amount of gas, the open crucible made of Al_2O_3 was destroyed and almost all of the K_2O must be removed from the open setup.

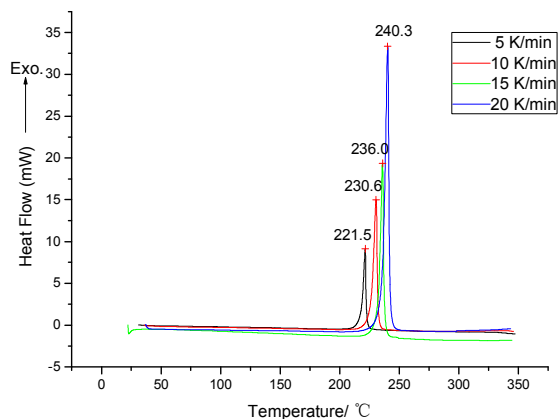


Fig. 5 DSC curves at different heating rates.

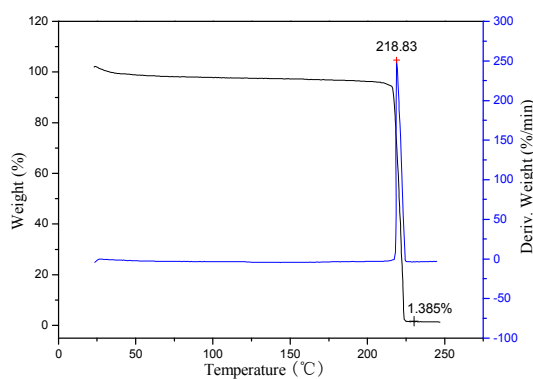


Fig. 6 TG/DTG curves of K_2BDFOF at the heating rate of 5 °C min^{-1} .

The impact sensitivity tests were carried out according to the

Fall Hammer Method using a 2.0 kg drop hammer on a ZBL-B

Table 2 Peak temperatures of the exothermic stage at different heating rates and the kinetic parameters

$\beta/K\text{ min}^{-1}$	$T_{pi}/\text{°C}$	$T_{po}/\text{°C}$	$T_b/\text{°C}$	$E_k/\text{kJ mol}^{-1[a]}$	$\log A_k/\text{s}^{-1[a]}$	$r_k^{[a]}$	$E_o/\text{kJ mol}^{-1[b]}$	$r_o^{[b]}$
5	221.5	205.8	219.3	148.0	15.19	0.9998	148.7	0.9999
10	230.6							
15	236.0							
20	240.3							

^[a] Subscript k, data obtained by Kissinger's method; ^[b] subscript o, data obtained by Ozawa's method.

The initial decomposition temperature (T_{p0}) is the peak temperature corresponding to $\beta = 0$, which can be obtained by substituting the T_{pi} and β_i from Table 3 into Equation (3).⁴²

$$T_{pi} = T_{p0} + b\beta_i + c\beta_i^2 + d\beta_i^3 \quad (3)$$

where b , c , d are coefficients.

The value of T_{p0} is obtained as 205.8 °C.

The critical temperature of thermal explosion (T_b) obtained from Equation (4) taken from references is 219.3 °C,⁴³ where the data of E_o is the apparent activation energy obtained by Ozawa's method.

impact sensitivity instrument. The friction sensitivity tests were carried out by using a Julius Peters machine using 20 mg sample. Compound K_2BDFOF is very sensitive towards impact (1-2 J) and friction (≤ 1 N), and because the value is comparable with lead azide, it should be considered to be a primary explosive; it should therefore only be handled with appropriate precautions.

3.4 Non-isothermal decomposition kinetics

In order to obtain the relative kinetic parameters such as activation energy (E), pre-exponential constant (A), entropy of activation (ΔS^\ddagger), enthalpy of activation (ΔH^\ddagger), and free energy of activation (ΔG^\ddagger), a multiple heating method (Kissinger's method and Ozawa's method) was employed.⁴⁰⁻⁴¹ The Kissinger and Ozawa equations are as follows:

$$\ln \frac{\beta_i}{T_{pi}^2} = \ln \frac{AR}{E_k} - \frac{E_k}{RT_{pi}} \quad (1)$$

$$\log \beta_i + \frac{0.4567 E_o}{RT_{pi}} = C \quad (2)$$

where T_p is the peak temperature; R is the gas constant (8.314 J mol^{-1}); A is the pre-exponential factor; E is the apparent activation energy; β is the linear heating rate and C is a constant.

Based on the exothermic peak temperatures measured at four different heating rates of 5, 10, 15, and 20 °C min^{-1} , the thermokinetic parameters of the complex were obtained. The apparent activation energies E_k and E_o , pre-exponential factor A_k and linear correlation coefficients R_k and R_o are shown in Table 2. From the results, we can see that the apparent activation energy obtained from Kissinger's method ($E_k = 148.0\text{ kJ mol}^{-1}$) is well consistent with that of Ozawa's method ($E_o = 148.7\text{ kJ mol}^{-1}$). Both of the linear correlation coefficients are all very close to 1, so the results are credible. Moreover, we can see that the activation energy (E) of the exothermic reaction is quite high, which also indicates that the title compound is quite stable.

$$T_b = \frac{E_o - \sqrt{E_o^2 - 4E_o RT_{p0}}}{2R} \quad (4)$$

With the data listed in Table 3, the entropy of activation (ΔS^\ddagger), enthalpy of activation (ΔH^\ddagger), and free energy of activation (ΔG^\ddagger) obtained by eqn (5) – (7) are 5.0 J mol^{-1} , 144.0 kJ mol^{-1} , and 141.6 kJ mol^{-1} , respectively.⁴⁴⁻⁴⁵

$$A = \frac{k_b T}{h} \exp\left(\frac{\Delta S^\ddagger}{R}\right) \quad (5)$$

$$\Delta H^\ddagger = E - RT \quad (6)$$

$$\Delta G^\ddagger = \Delta H^\ddagger - T\Delta S^\ddagger \quad (7)$$

where $T = T_{p0}$, the peak temperature (T_{pi}) corresponding to $\beta = 0$; $E = E_k$, calculated by Kissinger's method; $A = A_k$, calculated by Kissinger's method; k_b , the Boltzmann constant, $1.3807 \times 10^{-23} \text{ J K}^{-1}$; h , the Plank constant, $6.626 \times 10^{-34} \text{ J s}^{-1}$.

3.5 Heats of formation

The heats of formation ($\Delta_f H$) are another important parameter that needs to be taken into consideration when designing energetic materials. However, it was not possible to carry out with bomb calorimetric measurements due to the explosive character of the compound which oftentimes leads to incorrect values due to explosion and incomplete combustion. It is commonly accepted that heats of formation are calculated theoretically, and even superior results are achieved; therefore, the heat of formation of K_2BDFOF was calculated with the atomization method (eqn (8)) using the Gaussian 09 program package at the CBS-4M level of theory and summarized in Table

Table 3 Heat of formation based on CBS-4M calculations

M	$-H_{(M,298)}/\text{a.u.}^{[a]}$	$\Delta_f H^\circ_{(g)}/\text{kJ mol}^{-1 [b]}$	$U_l/\text{kJ mol}^{-1 [c]}$	$\Delta H_l/\text{kJ mol}^{-1 [d]}$	$\Delta_f H^\circ_{(s)}/\text{kJ mol}^{-1 [e]}$	$\Delta_f U^\circ_{(s)}/\text{kJ kg}^{-1 [f]}$
K^+	599.035967					
BDFOF anion	1827.557301					
K_2BDFOF		1145.1	1149.8	1153.5	-8.4	45.6

^[a] CBS-4M electronic enthalpy; ^[b] gas phase enthalpy of formation; ^[c] Lattice energy. ^[d] Lattice enthalpy ^[e] standard solid state enthalpy of formation; ^[f] solid state energy of formation.

3.6 Detonation parameters

The most important criteria of a high-initiation-power primary explosive are its detonation velocity V , and its detonation pressure P . In order to explore the performance of K_2BDFOF , these detonation parameters were calculated with the EXPLO5.05 software code and compared to those of lead azide and K_2DNABT .⁴⁸ The calculations were performed using the theoretical maximum densities at room temperatures. The crystal density of K_2BDFOF calculated at 296 K is 2.09 g cm^{-3} , which is comparable with K_2DNABT (2.11 g cm^{-3}). As can be seen in Table 4, the high density of K_2BDFOF with a good oxygen balance yields a remarkably high detonation pressure (329 kbar) and detonation velocity (8431 m s^{-1}). The calculated detonation pressure (329 kbar) of K_2BDFOF is in the range of lead azide, and easily outperform K_2DNABT . The detonation velocity of K_2BDFOF was calculated to be outstandingly high, which are strongly dependent on the oxygen balance of explosives. Therefore, K_2BDFOF displayed excellent integrated performance as a suitable and non-toxic replacement for lead azide, which is comparable with those of K_2DNABT .

Table 4 Physicochemical properties and detonation parameters of K_2BDFOF compared with those of lead azide and K_2DNABT

X	$\text{Pb}(\text{N}_3)_2$	K_2DNABT	K_2BDFOF
Formula	N_6Pb	$\text{C}_2\text{K}_2\text{N}_{12}\text{O}_4$	$\text{C}_8\text{K}_2\text{N}_{10}\text{O}_{13}$
$M [\text{g mol}^{-1}]$	291.3	334.3	522.4
$IS/J^{[a]}$	2.5–4	1	1–2
$FS/N^{[b]}$	0.1–1	≤ 1	≤ 1
$N/\%^{[c]}$	28.9	50.3	26.8
$N + O/\%^{[d]}$	28.9	69.4	66.6
$\Omega(\text{CO})/\%^{[e]}$	-11.0	4.8	12.3
$\Omega(\text{CO}_2)/\%^{[f]}$	-11.0	-4.8	-12.3
$T_{dec}/^\circ\text{C}^{[g]}$	315	200	221.5

3.³¹

$$\Delta_f H^\circ_{(g,M,298)} = H_{(Molecule,298)} - \sum H^\circ_{(Atoms,298)} + \sum \Delta_f H^\circ_{(Atoms,298)} \quad (8)$$

The lattice energy (U_l) and lattice enthalpy (ΔH_l) were calculated from the corresponding X-ray molecular volume according to the equation provided by Jenkins and Glasser.⁴⁶⁻⁴⁷ With the calculated lattice enthalpy the gas-phase enthalpy of formation $\Delta_f H^\circ_{(g,M)}$ was converted into the solid state (standard conditions) enthalpy of formation ΔH_l ($\Delta_f H^\circ_{(s,M)}$) by using the Jenkins' equations for X_2Y salts (for ionic derivatives).⁴⁶ These molar standard enthalpies of formation (ΔH_m) were used to calculate the molar solid state energies of formation (ΔU_m) according to equation (9).

$$\Delta U_m = \Delta H_m - \Delta n RT \quad (9)$$

in which Δn is the change of mol of gaseous components.

$\rho/\text{g cm}^{-3 [h]}$	4.8	2.11	2.09
$\Delta_f H^\circ/\text{kJ mol}^{-1 [i]}$	450.1	326.4	-8.4
$\Delta_f U^\circ/\text{kJ kg}^{-1 [j]}$	1574.9	1036.1	45.6
$P/\text{kbar}^{[k]}$	334.2	288.9	329.3
$V/\text{m s}^{-1 [l]}$	5876.8	8055.2	8430.9

^[a] Impact sensitivity; ^[b] Friction sensitivity; ^[c] Nitrogen content; ^[d] Combined nitrogen and oxygen content; ^[e] Oxygen balance assuming the formation of CO ; ^[f] Oxygen balance assuming the formation of CO_2 ; ^[g] Temperature of decomposition according to DSC (onset temperatures at a heating rate of 5°C min^{-1}); ^[h] Density at RT; ^[i] Heat of formation; ^[j] Energy of formation; ^[k] Detonation pressure; ^[l] Detonation velocity.

3.7 NBO analysis

To obtain a better understanding of structure for the anion, the natural bond orbital (NBO) as well as the molecular orbital analyses of BDFOF anion were carried out based upon the B3LYP/6-311+g(d, p) method with optimized structure. NBO analysis provides an efficient method for investigating charge distribution in molecular systems. As shown in Fig. 7. The NBO analysis indicated that the negative charge of $(\text{NO}_2)_2\text{C}^-$ is delocalized over the $\text{C}(\text{NO}_2)_2$ group, in which the charges of C(4) (0.087 e) and C(24) (0.087 e) are positive rather than negative. In the rings, carbon atoms bonded to O13 and O19 (C10, C14, C16, and C20) (0.432–0.467 e) are significantly higher than C6 (0.090 e) and C22 (0.090 e), which may be caused by the electron-withdrawing effect of oxygen atoms in the ether bonds. All of the ring nitrogen atoms (N9, N12, N15, N18, N21, and N23) (–0.080– –0.185 e) have negative charge densities, whereas the nitrogen atoms of the nitro groups (N1, N5, N26, and N27) (0.442–0.445e) have substantially positive charge density.

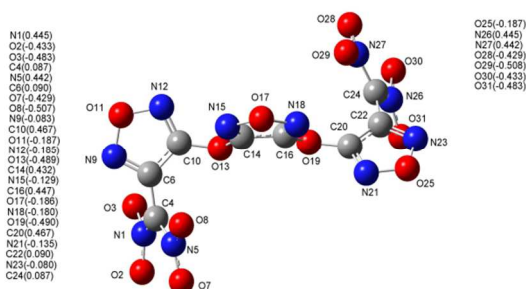


Fig. 7 Optimized structure and charge distribution in BDFOF anion as found with NBO analysis [B3LYP/6-311+G(d,p)].

The highest occupied molecular orbitals (HOMOs) and lowest unoccupied molecular orbitals (LUMOs) of the BDFOF anion (Fig. 8) further reveal that the dinitromethanide anions and its adjacent furazans occupy the HOMO, while the whole molecule of the anion occupy the LUMO. The negative charge is delocalized over the furazans. Since the gap energy of the highest occupied molecular orbitals and the lowest unoccupied molecular orbitals (ΔE) is an important parameter to measure the stability of the energetic material, the highest occupied molecular orbital energy (E_{HOMO}), the lowest unoccupied molecular orbital energy (E_{LUMO}) and their gaps (ΔE) were obtained as -0.06150 , 0.10088 and 0.16238 Hartree, respectively. It indicates that BDFOF anion has a better thermal stability. The conjugated charge distribution and acceptable ΔE likely cause the reasonable thermal stabilities.

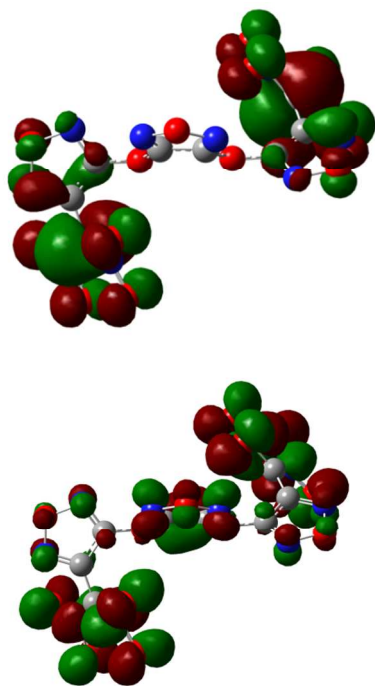


Fig. 8 The highest occupied molecular orbital (HOMO, top) and the lowest unoccupied molecular orbital (LUMO, bottom) of BDFOF anion.

4 Conclusions

From this experimental and theoretical study the following conclusions can be drawn:

Dipotassium 3,4-bis(3-dinitromethylfurazan-4-oxy)furazan (K_2 -

BDFOF) was synthesized in four steps for the first time. The single-crystal X-ray diffraction indicates that K_2 BDFOF was crystallized in a triclinic system, space group $P1$ with a high calculated density of 2.09 g cm^{-3} .

A violent decomposition was observed at $221.5 \text{ }^\circ\text{C}$, representing fast-detonation performance and superior thermostability. Additionally, K_2 BDFOF was found to have impact sensitivity of 1 J and friction sensitivity of 1 N that are in the range of lead azide and K_2 DNABT.

The calculated thermal dynamic parameters of K_2 BDFOF were obtained as follows: E_{k} , $148.0 \text{ kJ mol}^{-1}$; E_{o} , $148.7 \text{ kJ mol}^{-1}$; ΔS^\ddagger , 5.0 J mol^{-1} ; ΔH^\ddagger , $144.0 \text{ kJ mol}^{-1}$ and ΔG^\ddagger , $141.6 \text{ kJ mol}^{-1}$.

The energetic properties (detonation velocity, pressure, etc.) were calculated using the EXPLO5.05 program, and K_2 BDFOF shows a remarkably high detonation velocity of 8431 m s^{-1} and a detonation pressure of 329 kbar , which are in the range of K_2 DNABT. In comparison with the commonly used lead azide, it shows suitable properties, in particular, its high initiation power and non-toxicity.

Acknowledgements

This investigation received financial assistance from the National Natural Science Foundation of China (Grant No. 21373157), Basal Science Foundation of National Defense (Grant No. B0920110005).

Notes and references

- ^a Xi'an Modern Chemistry Research Institute, Xi'an 710069, P. R. China. E-mail: xuezhongfan@126.com; Fax: +86-02 9-88291306; Tel: +86-029-88291306
- ^b School of Chemical Engineering and the Environment, Beijing Institute of Technology, Beijing 100081, P. R. China
- † Electronic Supplementary Information (ESI) available: The CIF file gives crystallographic data for the complex. CCDC 966224. For ESI and crystallographic data in CIF or other electronic format see DOI: 10.1039/b000000x/
- N. Mehta, K. Oyler, G. Chemg, A. Shah, J. Marin, and K. Yee, *Z. Anorg. Allg. Chem.*, 2014, **640**, 1309.
 - T. M. Klapötke, *Propellants Explos. Pyrotech.*, 2014, **39**, 7.
 - D. M. Badgajar, M. B. Talawar, S. N. Asthana, P. P. Mahulikar, *J. Hazard. Mater.*, 2008, **151**, 289.
 - Q. H Zhang and J. M. Shreeve, *Angew. Chem. Int. Ed.*, 2014, **53**, 2540.
 - X. Y. Liu, Q. Yang, Z. Y. Su, S. P. Chen, G. Xie, Q. Wei, and S. L. Gao, *RSC Adv.*, 2014, **4**, 16087.
 - D. Izsák, T. M. Klapötke, S. Reuter, *Eur. J. Inorg. Chem.*, 2013, 5641.
 - R. F. Wu, Y. J. Zhu, and W. Jin, *Z. Anorg. Allg. Chem.*, 2013, **639**, 2290.
 - M. Joas, T. M. Klapötke, J. Stierstorfer, and N. Szimhardt, *Chem. Eur. J.*, 2013, **19**, 9995.
 - T. M. Klapötke, *Chemistry of High-Energy Materials*, 2ednd edWalter de Gruyter, Berlin, 2012, p. 19.
 - F. C. Tompkins, D. A. Young, *J. Chem. Soc.*, 1956, 3331.
 - R. Matyas, and J. Pachman. 2013. *Primary Explosives*. Heidelberg, Germany: Springer.
 - J. Akhavan, *Chemistry of Explosives*, 3rd ed., The Royal Society of Chemistry, Cambridge, UK, 2011, p 35.
 - N. Fischer, M. Joas, T. M. Klapötke, and J Stierstorfer, *Inorg. Chem.*, 2013, **52**, 13791.
 - T. Musil, R. Matyas, R. Vala, A. Ruzicka, and M. Vlcek, *Propellants Explos. Pyrotech.*, 2014, **39**, 251.
 - R. A. Faust, *Toxicity Summary for Silver*, 1992, Center for Integrated Risk Assessment, Oak Ridge National Laboratory, <http://cira.ornl.gov>.
 - J. W. Fronabarger, M. D. Williams, W. B. Sanborn, J. G. Bragg, A. P. Damon, and M. Bichay, *Propellants Explos Pyrotech.*, 2011, **36**, 541.

- 17 S. H. Li, Y. Wang, C. Qi, X. X. Zhao, J. C. Zhang, S. W. Zhang, and S. P. Pang, *Angew. Chem. Int. Ed.*, 2013, **52**, 14031.
- 18 R. J. Irwin, Environmental Contaminants Encyclopedia: Copper, 1997, National Park Service, <http://www.nature.nps.gov>.
- 5 19 H. Brand, P. Mayer, K. Polborn, A. Schulz, J. J. Weigand, *J. Am. Chem. Soc.*, 2005, **127**, 1360.
- 20 C. M. Sabaté, E. Jeanneau and H. Delalu, *Dalton Trans.*, 2012, **41**, 3817.
- 21 J. W. Fronabarger, M. D. Williams, W. B. Sanborn, D. A. Parrish, M. Bichay, *Propellants Explos. Pyrotech.*, 2011, **36**, 459.
- 10 22 D. Fischer, T. M. Klapötke, and J. Stierstorfer, *Angew. Chem. Int. Ed.*, 2014, **53**, 8172.
- 23 A. B. Sheremetev, *J. Heterocyclic. Chem.*, 1995, **32**, 371.
- 24 A. B. Sheremetev, V. O. Kulagina, N. S. Aleksandrova, D. E. Dmitriev, Y. A. Strelenko, *Propellants, Expl. Pyrotechn.*, 1998, **23**, 142.
- 15 25 L. X. Liang, H. F. Huang, K. Wang, C. M. Bian, J. H. Song, L. M. Ling, F. Q. Zhao, and Z. M. Zhou, *J. Mater. Chem.*, 2012, **22**, 21954.
- 26 A. B. Sheremetev, S. E. Semenov, V. S. Kuzmin, Y. A. Strelenko, and S. L. Ioffe, *Chem. Eur. J.*, 1998, **4**, 1023.
- 20 27 X. J. Wang, K. Z. Xu, Q. Sun, B. Z. Wang, C. Zhou, and F. Q. Zhao, *Propellants Explos. Pyrotech.*, 2015, **40**, 9.
- 28 Y. S. Zhou, K. Z. Xu, B. Z. Wang, H. Zhang, Q. Q. Qiu, F. Q. Zhao, *Bull. Korean Chem. Soc.*, 2012, **33**, 3317.
- 29 H. Li, F. Q. Zhao, B. Z. Wang, L. J. Zhai, W. P. Lai, N. Liu, A new family of energetic salts based on oxy-bridged bis(dinitromethyl)furazan: syntheses, characterization and properties, *RSC Adv.*, 2015, DOI:10.1039/C5RA00175G
- 25 30 R. Meyer and J. Kohler, Explosives, ed. Revised and extended, VCH Publishers, New York, 4th edn, 1993, vol. 197.
- 30 31 M. J. Frisch, G. W. Trucks, H. B. Schlegel, G. E. Scuseria, M. A. Robb, J. R. Cheeseman, J. A. Montgomery Jr., T. V.reven, K. N. Kudin, J. C. Burant, J. M. Millam, S. S. Iyengar, J. Tomasi, V. Barone, B. Mennucci, M. Cossi, G. Scalmani, N. Rega, G. A. Petersson, H. Nakatsuji, M. Hada, M. Ehara, K. Toyota, R. Fukuda, J. Hasegawa, M. Ishida, T. Nakajima, Y. Honda, O. Kitao, H. Nakai, M. Klene, X. Li, J. E. Knox, H. P. Hratchian, J. B. Cross, V. Bakken, C. Adamo, J. Jaramillo, R. Gomperts, R. E. Stratmann, O. Yazyev, A. J. Austin, R. Cammi, C. Pomelli, J. W. Ochterski, P. Y. Ayala, K. Morokuma, G. A. Voth, P. Sal-vador, J. J. Dannenberg, V. G. Zakrzewski, S. Dapprich, A. D. Daniels, M. C. Strain, O. Farkas, D. K. Malick, A. D. Rabuck, K. Raghavachari, J. B. Foresman, J. V. Ortiz, Q. Cui, A. G. Ba-boul, S. Clifford, J. Cioslowski, B. B. Stefanov, G. Liu, A. Lia-shenko, P. Piskorz, I. Komaromi, R. L. Martin, D. J. Fox, T. Keith, M. A. Al-Laham, C. Y. Peng, A. Nanayakkara, M. Challacombe, P. M. W. Gill, B. Johnson, W. Chen, M. W. Wong, C. Gonzalez, J. A. Pople. 2009. Gaussian 09, rev. A.02, Gaussian, Inc., Wallingford CT.
- 40 45 32 GaussView 5, V5.0.8, T. K. R. Dennington, J. Millam, Semichem Inc., Shawnee Mission, 2009.
- 33 J. J. A. Montgomery, M. J. Frisch, J. W. Ochterski, G. A. Petersson, *J. Chem. Phys.*, 2000, **112**, 6532.
- 50 34 J. W. Ochterski, G. A. Petersson, J. J. A. Montgomery, *J. Chem. Phys.*, 1996, **104**, 2598.
- 35 E. F. C. Byrd, B. M. Rice, *J. Chem. Phys.*, 2005, **110**, 1005.
- 36 L. A. Curtiss, K. Raghavachari, P. C. Redfern, J. A. Pople, *J. Chem. Phys.*, 1997, **106**, 1063.
- 55 37 G. M. Sheldrick, SHELXS-97, Program for X-ray Crystal Structure Determination, University of Göttingen, Germany, 1997.
- 38 O. A. Lukyanov, and T. I. Zhiguleva, *Bulletin of the Academy of Sciences of the USSR*, 1982, **31**, 1270.
- 60 39 O. A. Lukyanov, and G. V. Pokhvisneva, *Bulletin of the Academy of Sciences of the USSR*, 1991, **40**, 2439.
- 40 H. E. Kissinger, *Anal. Chem.* 1957, **29**, 1702.
- 41 T. Ozawa, *Bull. Chem. Soc. Jpn.* 1965, **38**, 1881.
- 42 R. Z. Hu, S. L. Gao, F. Q. Zhao, Q. Z. Shi, T. L. Zhang, J. J. Zhang, Thermal Analysis Kinetics, 2nd ed., Science Press, Beijing, 2008.(in Chinese).
- 65 43 T. L. Zhang, R. Z. Hu, Y. Xie, F. P. Li, *Thermochim. Acta*, 1994, **244**, 171.
- 44 M. Najafi and A. K. Samangani, *Propellants Explos. Pyrotech.*, 2011, **36**, 487.
- 70 45 R. Z. Hu, S. P. Chen, S. L. Gao, F. Q. Zhao, Y. Luo, H. X. Gao, Q. Z. Shi, H. A. Zhao, P. Yao and J. Li, *J. Hazard. Mater.*, 2005, **117**, 103.
- 46 H. D. B. Jenkins, D. Tudela and L. Glasser, *Inorg. Chem.*, 2002, **41**, 2364.
- 75 47 H. D. B. Jenkins, H. K. Roobottom, J. Passmore and L. Glasser, *Inorg. Chem.*, 1999, **38**, 3609.
- 48 M. Sucińska, Brodarski Institute, Zagreb, Croatia, EXPLOS 5.05 program, 2006.